INT. J. NUM. METH. HEAT FLUID FLOW, VOL. 3, 341–355 (1993)

LAMINAR FULLY DEVELOPED INCOMPRESSIBLE FLOW WITH MIXED CONVECTION IN INCLINED TUBES

J. ORFI AND N. GALANIS

Faculté des Sciences Appliquées, Université de Sherbrooke, Sherbrooke (Québec) J1K 2R1, Canada

AND

C. T. NGUYEN

École de Génie, Université de Moncton, Moncton (N.B.) E1A 3EP, Canada

ABSTRACT

The effects of tube inclination and Grashof number on the fully developed hydrodynamic and thermal fields are investigated numerically for laminar ascending flow of air and water in uniformly heated circular tubes. The effects of the buoyancy induced secondary flow on the hydrodynamic and thermal fields are complex and strongly dependent on the Grashof number, the Prandtl number and the tube inclination. The influence of these parameters on the intensity of the secondary flow, on the distortion of the axial velocity profile and of the temperature field from the corresponding distributions for pure forced flow, as well as on the circumferential variation of the local shear stress and of the local Nusselt number are analysed. The average shear stress is higher than for pure forced flow and it increases with both the tube inclination and with the Grashof number. The average Nusselt number is higher than for pure forced flow and increases with the Grashof number. For a given fluid and Grashof number there exists an optimum tube inclination which maximizes the average Nusselt number. Correlations for the average Nusselt number in terms of Gr and Pr are presented for four different tube inclinations.

KEY WORDS Laminar flow Shear stress SIMPLER method

NOMENCLATURE

A	non-dimensional coefficient in (13)
b, c	non-dimensional exponents in (13)
c_p	specific heat of the fluid (J/kg K)
Gr	Grashof number (defined in (10))
g	local acceleration due to gravity (m/s^2)
k	thermal conductivity of the fluid (W/m K)
Nu	local Nusselt number (function of θ); a bar over this symbol defines the average circumferential Nusselt number
P	local pressure (function of r, θ, z); a bar over this symbol defines the average pressure in a cross-sectional normal to the tube axis
Pr	Prandtl number
q''	rate of heat flux at the wall (W/m^2)
R	inside radius of the tube (m)
Ra	Rayleigh number
Re	Reynolds number (defined in (10))
r	non-dimensional radial coordinate
S	non-dimensional source term in momentum and energy equations
T	non-dimensional fluid temperature
T_w	fluid temperature at $r=1$ (function of θ); a bar over this symbol defines the average wall temperature
V_0	average axial velocity (m/s)
V	non-dimensional fluid velocity
z	non-dimensional axial coordinate

0961–5539/93/040341–15$2.00

Received April 1992
Revised March 1993

Greek letters

α	tube inclination (degrees from horizontal)
β	expansion coefficient of the fluid (K^{-1})
ΔT^*	reference temperature difference ($\Delta T^* = q''.R/k$)
θ	angular coordinate (degrees from vertical)
μ	fluid viscosity (N s/m^2)
ν	fluid kinematic viscosity (m^2/s)
τ	non-dimensional shear stress at $r=1$ (function of θ); a bar over this symbol defines the average circumferential shear stress
ψ	non-dimensional stream function for the secondary flow

Indices

r, θ, z	define respectively the radial, angular, axial components
min, max	define respectively the minimum, maximum value of a variable

INTRODUCTION

Laminar flow with combined forced and free convection occurs in different thermal applications such as heat exchangers, solar collectors, pipelines and nuclear reactors. In such situations two symmetrical vortices are generated as warm fluid rises near the wall under the effect of buoyancy. The axisymmetry of the flow field is destroyed and isotherms are drastically different from the concentric circles corresponding to pure forced flow. Nguyen and Galanis[1,2] have presented detailed numerical results for the simultaneously developing hydrodynamic and thermal boundary layers in horizontal uniformly heated tubes.

In this paper we investigate the effect of tube inclination, as well as that of the Grashof and Prandtl numbers, on the fully-developed flow in uniformly heated tubes. For this thermal boundary condition, the vortices generated by natural convection persist over the entire heated length of the tube. This is not the case for uniform temperature tubes, since in this case the fluid reaches a uniform temperature and natural convection effects disappear in the fully-developed region.

The problem under study has been investigated experimentally[3–5] but exhaustive results are available only for horizontal and vertical tubes. It has also been treated analytically with various approaches which did not always give satisfactory agreement with measured values. Thus, the perturbation technique[6] gives unrealistically high estimates of the Nusselt number even at moderate values of the Rayleigh number. Boundary layer solutions[7] seem to be valid only for relatively large Rayleigh numbers. The boundary–vorticity method[8] has also been used. The literature includes certain contradictory results with respect to the influence of tube inclination on the Nusselt number: some authors[6] conclude that there exists an optimum tube inclination which maximizes the Nusselt number while experimental and analytical results by others[5,8] do not confirm this result. The present authors have addressed this problem for the case of air[9] and have discussed in detail the effects of the Grashof number on the flow and thermal fields in the case of that same fluid[10].

MODELLING AND SIMULATION

The problem considered is the fully-developed ascending laminar flow under combined forced and free convection inside an inclined circular tube with uniform heat flux q'' at the wall (*Figure 1*). All properties of the fluid are assumed constant except for the density in the buoyancy terms (Boussinesq's assumption). The heat generation due to viscous dissipation is neglected. Furthermore, in the fully-developed region the following conditions must be respected:

—no axial gradient for any velocity component;

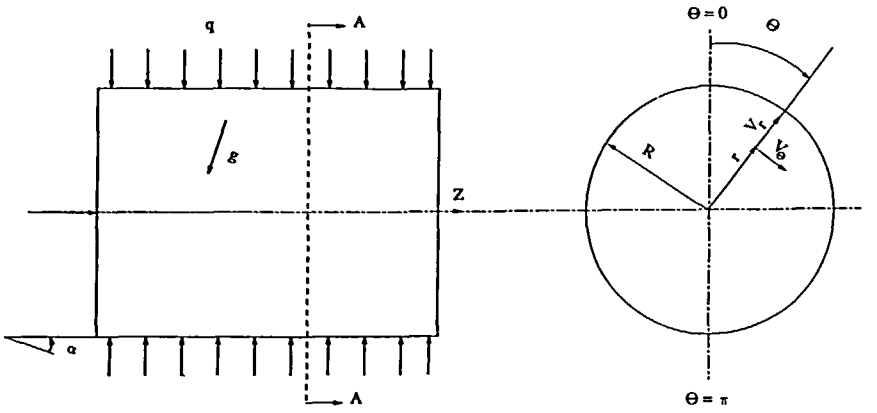

Figure 1 Schematic representation of the problem under study

—constant uniform axial pressure gradient (this quantity is unknown and must be calculated as part of the solution);
—constant uniform axial gradient for the fluid temperature (this quantity is known and is proportional to the imposed wall heat flux q'').

With these considerations, the dimensionless governing equations (mass, momentum and energy) in cylindrical coordinates are as follows:

$$\frac{\partial(rV_r)}{\partial r}+\frac{\partial V_\theta}{\partial \theta}=0 \tag{1}$$

$$V_r\frac{\partial V_\theta}{\partial r}+\frac{V_\theta}{r}\frac{\partial V_\theta}{\partial \theta}=-\frac{1}{r}\frac{\partial P}{\partial \theta}+\frac{1}{Re}\nabla^2 V_\theta+S_\theta \tag{2}$$

$$V_r\frac{\partial V_r}{\partial r}+\frac{V_\theta}{r}\frac{\partial V_r}{\partial \theta}=-\frac{\partial P}{\partial r}+\frac{1}{Re}\nabla^2 V_r+S_r \tag{3}$$

$$V_r\frac{\partial V_z}{\partial r}+\frac{V_\theta}{r}\frac{\partial V_z}{\partial \theta}=\frac{1}{Re}\nabla^2 V_z+S_z \tag{4}$$

$$V_r\frac{\partial T}{\partial r}+\frac{V_\theta}{r}\frac{\partial T}{\partial \theta}=\frac{1}{RePr}\nabla^2 T+S_e \tag{5}$$

The source terms for the momentum and energy equations are respectively:

$$S_\theta=-\frac{V_rV_\theta}{r}+\frac{1}{Re}\left[\frac{2}{r^2}\frac{\partial V_r}{\partial \theta}-\frac{V_\theta}{\partial \theta}-\frac{V_\theta}{r^2}\right]-\frac{Gr}{Re^2}T\cos\alpha\sin\theta \tag{6}$$

$$S_r=\frac{V_\theta^2}{r}+\frac{1}{Re}\left[-\frac{V_r}{r^2}-\frac{2}{r^2}\frac{\partial V_\theta}{\partial \theta}\right]+\frac{Gr}{Re^2}T\cos\alpha\cos\theta \tag{7}$$

$$S_z=-\frac{d\bar{P}}{dz}+\frac{Gr}{Re^2}T\sin\alpha \tag{8}$$

$$S_e=-2V_z/(Re\ Pr) \tag{9}$$

In the above equations, the velocity components are non-dimensionalized with respect to the mean axial velocity V_0, the pressure with respect to the quantity ρV_0^2 and all lengths with respect

to the tube radius R. The non-dimensional temperature represents the difference between the local value and the bulk temperature in the corresponding cross-section divided by $\Delta T^* = q''R/k$ (k is the fluid conductivity). The governing dimensionless parameters are defined as:

$$Re = V_0 R/\nu \qquad Gr = g\beta R^3 \Delta T^*/\nu^2 \qquad Pr = c_p \mu/k \tag{10}$$

It is important to note that in the source term S_z (8) of the axial momentum equation, the pressure gradient, which in general depends on r, θ, and z, has been replaced by the corresponding axial gradient of the cross-sectional average pressure $d\bar{P}/dz$. The latter is obviously independent of r and θ. Furthermore, for a fully-developed flow which is the case studied here, this pressure gradient $d\bar{P}/dz$ is in fact a constant for a given set of Gr, Re, Pr, and α values. The use of the axial gradient of the average pressure instead of the local pressure gradient has been originally proposed by Patankar and Spalding[11] for three-dimensional parabolic flow problems. This approach was later extended and widely used for other situations, in particular for fully developed internal flows with mixed convection[12,13].

It should also be noted that for vertical tubes ($\alpha = 90°$) the flow is one-dimensional ($V_r = V_\theta = 0$) since the buoyancy force acts in the axial direction. For this geometry, (1) is trivial, (2) and (3) show that the pressure is independent of r and θ, while the left hand side of (4) and (5) are identically zero. The simplified set of equations resulting by replacing S_z from (8) in (4) and S_e from (9) in (5) is independent of the Prandtl number. Thus for vertical tubes, the hydrodynamic and thermal fields depend only on the Reynolds and Grashof numbers; they are the same for all fluids. This property of flow in vertical tubes has also been reported by Iqbal and Stachiewicz[6] and Petukhov *et al.*[4].

The governing equations constitute a highly coupled system. They are subjected to the usual hydrodynamic (no slip) and thermal (uniform radial temperature gradient) conditions at the wall. The numerical method employed to solve the problem is based on the SIMPLER method[14]. The pressure equation and the pressure-correction equation have been derived from the continuity and momentum equations; the first calculates the pressure field $P(r, \theta)$ in the domain for a guessed velocity field and an arbitrary value of the unknown axial pressure gradient, while the second performs necessary corrections on the velocities in order to satisfy mass conservation. It is important to note that according to the SIMPLER method[14], and for the problem under study for which all velocity components on the boundaries are given, there is no need to specify the corresponding pressures. Furthermore, only pressure differences rather than absolute values are relevant. Once convergence is achieved, the average axial non-dimensional velocity is evaluated; if it is different than unity, i.e. if the overall mass balance is not satisfied, the whole procedure is repeated for a new value of the unknown axial pressure gradient. This iterative procedure finally results in a coherent solution giving the temperature, velocity and pressure distributions in a section normal to the tube axis, as well as the axial variation of the pressure.

Since the flow field is symmetrical about the vertical diameter the solution must only be calculated over half of the circular cross-section. Several different grids were used to insure that the results are independent of the number of nodes used in the discretization process. *Table 1* shows the effect of grid size on the computed average Nusselt number for $Gr = 1000$, $Pr = 0.7$, $Re = 250$ and a horizontal tube ($\alpha = 0°$). The computed axial velocity profile and temperature

Table 1 Effect of grid size on average Nusselt number

Number of grip points in tangential direction	Number of grid points in radial direction	$\overline{Nu}$
15	17	4.82
17	21	4.81
25	28	4.80
29	30	4.80

distribution along the vertical diameter for two grids (29×30 and 35×35) were also compared and found to be identical for all practical purposes[15]. In light of those results all further calculations were performed with the 29×30 grid.

The computer program has also been successfully validated by comparing the numerical results with the analytical solution for the limiting case of negligible buoyancy forces. Both velocity and temperature profiles as well as the Nusselt number and axial pressure gradient agree exceptionally well with the analytical values[15].

RESULTS AND DISCUSSION

For the combined forced and free convection, numerical simulations have been performed for two fluids (air, $Pr=0.7$ and water, $Pr=7$), a Reynolds number of 250, tube inclinations ranging from $\alpha=0°$ (horizontal) to $\alpha=90°$ (vertical), and several values of the Grashof number resulting in a Rayleigh number range extending from zero to 2.1×10^6. In order to illustrate the effects of the Grashof number, the tube inclination and the Prandtl number, some typical results are presented in the following sections.

Velocity and thermal fields

Axial velocity profiles. Figures 2a and *2b* show the effects of the Grashof number on the axial velocity profile along the vertical diameter $\theta=0$, π for $Pr=7$ and $\alpha=0°$, $\alpha=60°$ respectively. Under the effects of natural convection, the symmetry of the flow field is destroyed and it becomes quite different from the one corresponding to pure forced flow ($Gr=0$). The maximum axial velocity does no longer occur on the tube centreline and is not always equal to 2.0. As shown by these Figures, the position and magnitude of the maximum axial velocity are affected by both the Grashof number and the tube inclination. For horizontal tubes, the maximum occurs below the centreline while for steeply inclined tubes and high Grashof numbers the maximum occurs above the centreline. This effect has also been reported by Nguyen[16] and by Iqbal and Stachiewicz[6]. This behaviour results from the effect of natural convection on the axial forced flow, which is quite different depending upon the tube inclination considered. For horizontal tubes, the buoyancy forces are perpendicular to the tube axis. The resulting secondary flow, which is more significant in the lower part of the tube (see *Figure 5*), pushes the fluid with high axial velocity towards the bottom of the tube. This explains why for horizontal tubes the

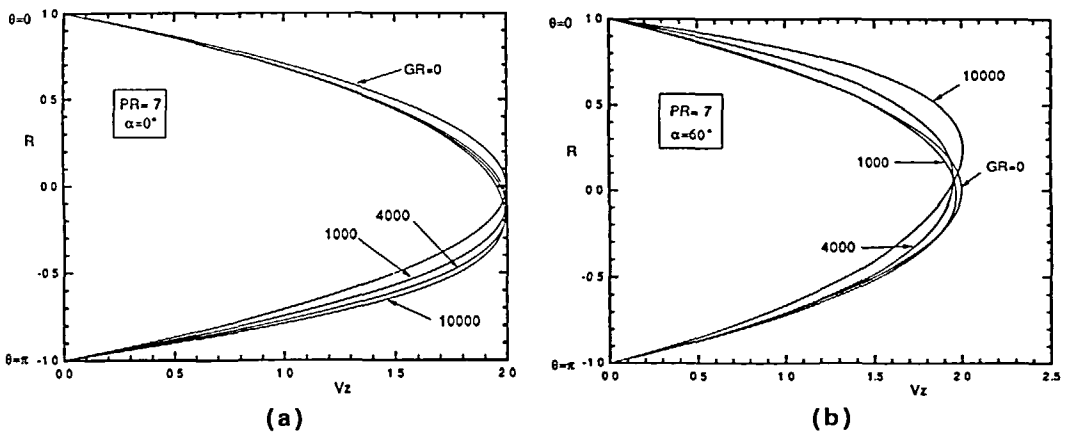

Figure 2 Effect of Grashof number on the axial velocity profile along the vertical diameter for water

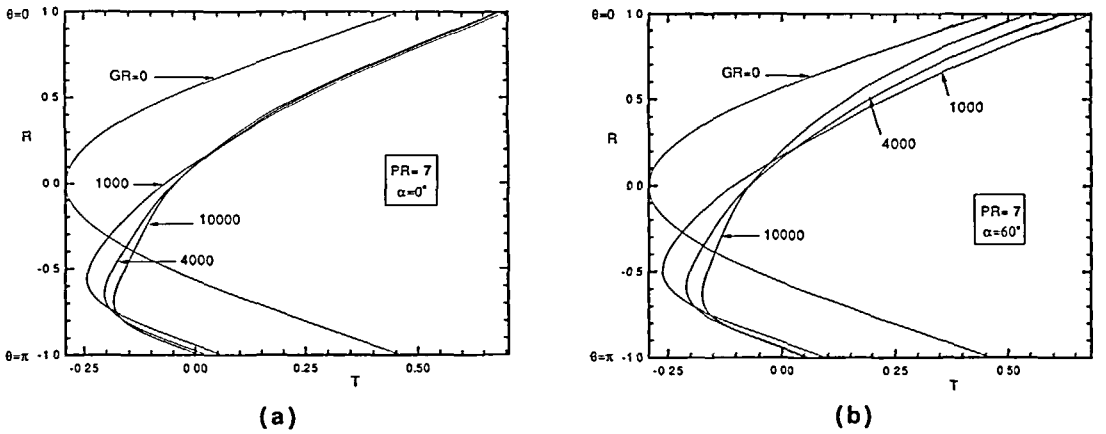

Figure 3 Effect of Grashof number on the water temperature profile along the vertical diameter

maximum axial velocity occurs below the centreline. Furthermore, in the upper region of the horizontal tube where the secondary flow is weak, the axial velocity profile is essentially independent of the Grashof number. On the other hand, for steeply inclined tubes ($\alpha=60°$ for example) the buoyancy forces act predominantly in the axial direction. Since these axial forces are more important in the upper part of the tube where the temperatures are higher (see *Figure 3b*), the axial velocity in this region is higher. For sufficiently high Grashof numbers, this can result in a maximum of the axial velocity well above the tube centreline.

In the case of vertical tubes ($\alpha=90°$), numerical results not shown here indicate that the axial velocity profile is, as expected, axisymmetric[15]. At low Grashof numbers the maximum axial velocity occurs on the tube centreline; but as the Grashof number increases (due to an increase of the imposed wall heat flux q''), the position of the maximum axial velocity moves outwards towards the wall and the fluid near the tube centreline becomes progressively slower. Similar results have been obtained by Cheng and Hong[8] and by Collins[17].

Fluid temperature profiles. Figures 3a and *3b* illustrate the effects of the Grashof number on the dimensionless water temperature profiles along the diameter $\theta=0$, 180° for $\alpha=0°$, $\alpha=60°$, respectively. These profiles are very different from the axisymmetric one corresponding to pure forced flow ($Gr=0$). The minimum field temperature occurs well below the centreline and moves progressively towards the lower wall as Gr increases. In the upper region of the tube ($r>0.25$) the dimensionless fluid temperature is for all practical purposes independent of Gr in the case of horizontal tubes since the secondary flow is almost non-existent in this region of the tube and, as stated earlier, the axial velocity profile is essentially independent of the Grashof number. This result indicates that the difference between the local and bulls temperatures increases proportionally with the increase of the Grashof number. In the case of steeply inclined tubes however, the dimensionless fluid temperature in the upper region decreases as the heat flux (and the Grashof number) increases due to the fact that the axial velocity profile in this region is considerably influenced by the Grashof number (see *Figure 2b*).

For vertical tubes the fluid temperature profile is axisymmetric. The difference between T_{max}, occurring at the wall, and T_{min}, occurring at the centre, decreases slightly as the Grashof number increases.

Wall temperature distribution. Figures 4a and *4b* illustrate the effects of the Grashof number on the angular distribution of the wall temperature for $\alpha=0°$, $\alpha=60°$ respectively. *Figure 4a* also provides a comparison of the numerically predicted wall temperature distribution for $\alpha=0°$,

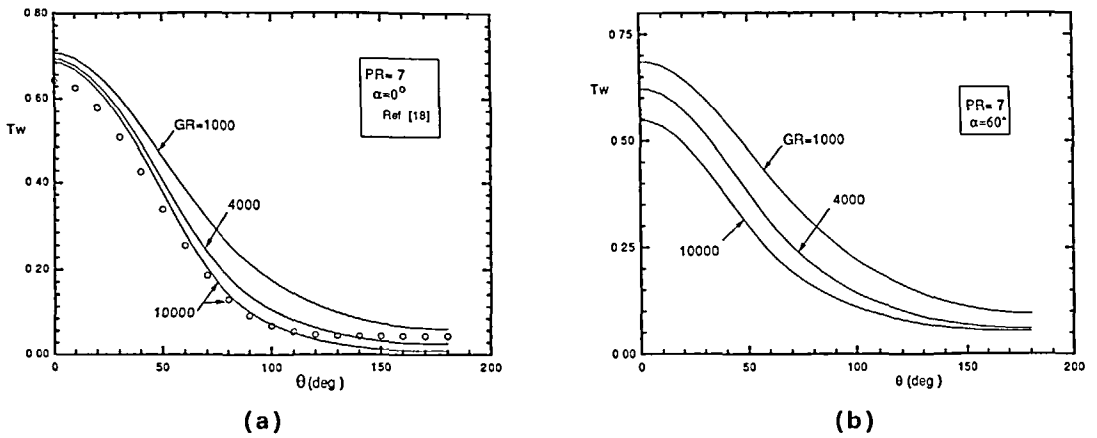

Figure 4 Effect of Grashof number on the angular distribution of the wall temperature for water

$\alpha = 60°$ respectively. *Figure 4a* also provides a comparison of the numerically predicted wall temperature distribution for $\alpha = 0°$, $Pr = 7$ and $Gr = 10{,}000$ with corresponding results from an experimental correlation by Petukhov and Polyakov[18]. Their agreement is quite acceptable. The calculated results indicate that the temperature difference between the top ($\theta = 0°$) and bottom ($\theta = 180°$) of the tube increases with the Grashof number, most notably for the horizontal tube. The circumferential variation of the wall temperature is particularly important in the upper region of the tube ($0 \leqslant \theta \leqslant 90°$) where the hot fluid resides. In the lower region of the tube, where the cold fluid is found, the wall temperature remains essentially uniform and its value decreases as the Grashof number increases. For sufficiently high values of the Grashof number, the wall temperature in the lower part of horizontal tubes is negative[15], i.e. lower than the fluid bulk temperature. This numerical prediction has been confirmed experimentally by Petukhov[4] and by Newel and Bergles[19].

Secondary flow structure and isotherms. In order to understand better the effects of natural convection, the streamlines and isotherms in a plane normal to the tube axis for $\alpha = 0°$, $Pr = 7$ and $Gr = 1000$, 4000, 10,000 are shown in *Figures 5a*, *5b* and *5c* respectively. We observe that, in general, the secondary flow is more important in the lower part of the cross-section. As the Grashof number increases the streamlines become more distorted and asymmetrical with respect to the horizontal diameter while their gradient in the vicinity of the tube wall becomes much more important than in the central and upper regions of the tube. Furthermore, the strength of the secondary flow, indicated by the maximum value of the stream function ψ_{max}, also increases considerably with the Grashof number. It is also observed that the vortex centre moves progressively downwards and slightly towards the tube wall as Gr increases.

The effects of natural convection on the thermal field are quite evident in *Figure 5*. All isotherms are distorted and quite different from the concentric circles which correspond to pure forced flow. It is interesting to observe that in the central and upper parts of the tube, temperature gradients are quite low. This explains the low intensity of the secondary flow in this region. In the lower part, however, particularly in the vicinity of the tube wall, the temperature gradient is important and, consequently, the corresponding secondary flow is intense. When the Grashof number increases, all these effects become more pronounced. Isotherms become more distorted, particularly in the central region where they are almost horizontal. The cold fluid zone (i.e. the zone where $T < 0$), as well as the position of the minimum fluid temperature, move slightly downwards. It is also important to mention that this effect on the position of the minimum

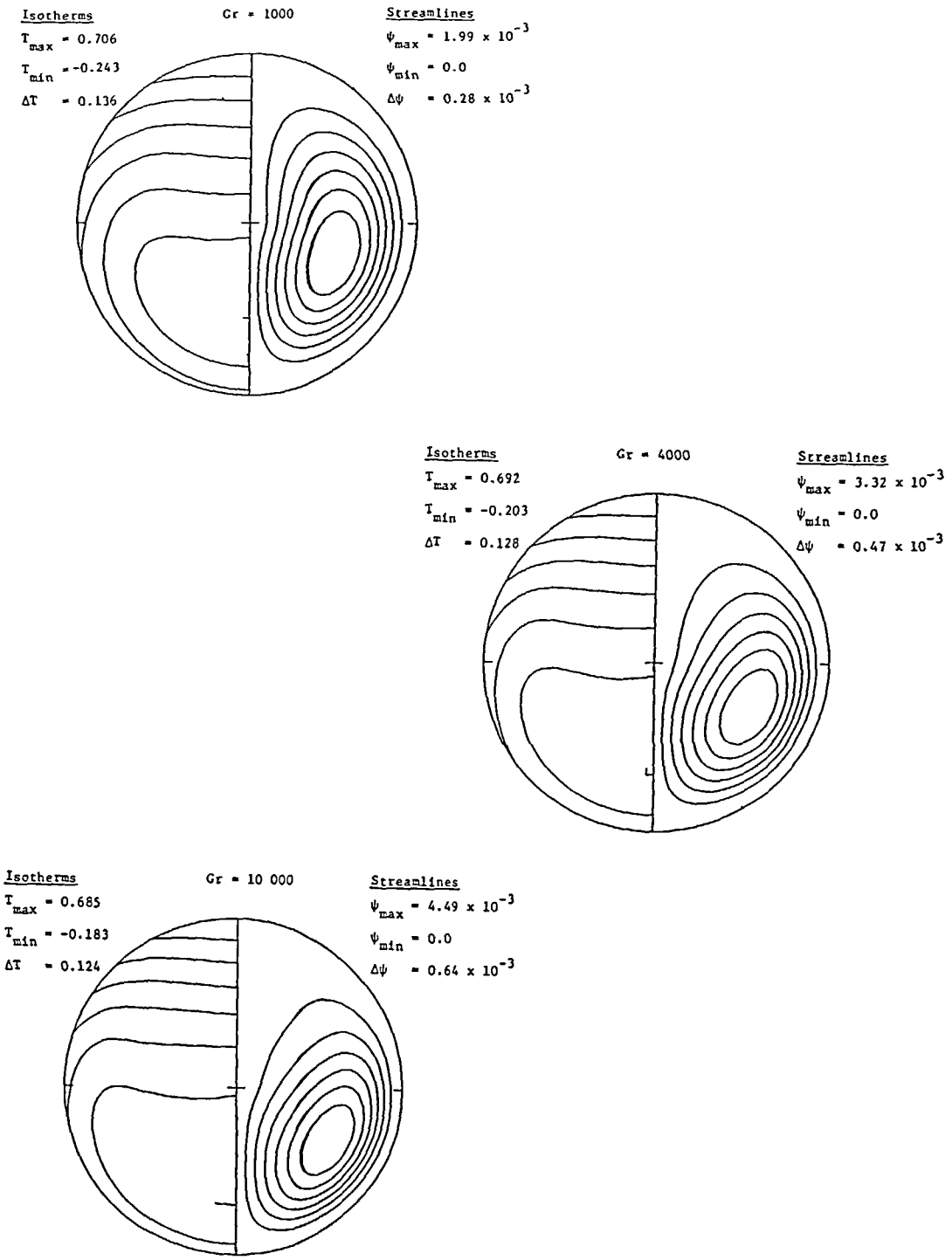

Figure 5 Isotherms and secondary flow streamlines in a plane normal to the tube axis for flow of water in a horizontal tube

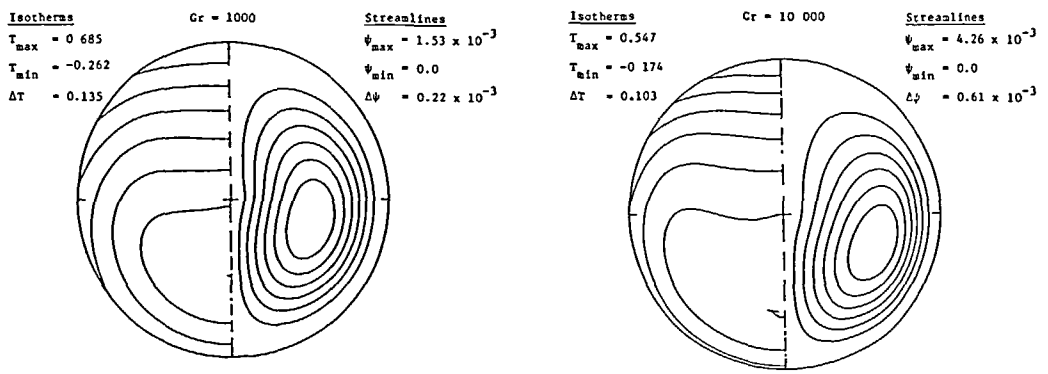

Figure 6 Isotherms and secondary flow streamlines in a plane normal to the tube axis for flow of water in an inclined tube ($\alpha = 60°$)

fluid temperature has been observed by several other researchers such as Nguyen[16], Siegwarth[20] and Hong[21]. The difference between the dimensionless maximum fluid temperature (located at the top of the tube, i.e. at $\theta = 0$, $r = 1$) and the corresponding minimum value increases with the Grashof number and is a clear indication of the importance of the secondary flow.

Similar trends on the influence of the Grashof number have been also obtained for inclined tubes[15]. *Figures 6a* and *6b* illustrate for example the secondary flow structure and isotherms for $\alpha = 60°$, $Pr = 7$ and a Grashof number of 1000 and 10,000 respectively.

Effects of Prandtl number on velocity and thermal fields. A comparison of the velocity and temperature profiles for water ($Pr = 7$) presented in *Figures 2* to *6* with corresponding results for air ($Pr = 0.7$) published previously[10] is quite interesting.

Thus, with respect to the axial velocity profile, it can be observed that the departure from the Poiseuille parabolic profile is much more significant for air. Indeed, for $\alpha = 0°$ and $Ra = 7 \times 10^3$, the maximum axial velocity for air is 1.94 and occurs at $r = -0.47$ while the corresponding values for water are 2.0 and $r = -0.06$. Similarly, for $\alpha = 60°$ and $Ra = 7 \times 10^3$ the maximum axial velocity for air is 1.76 and occurs at $r = 0.07$ while the corresponding values for water are 1.96 and 0.02. This observation concerning the effect of the Prandtl number on the primary flow field is confirmed for all tube inclinations and for the whole range of Gr, or Ra, under consideration. By extension, it can be argued that as the Prandtl number increases, the axial velocity profile for all tube inclinations and Grashof numbers tends to the axisymmetric Poiseuille profile. This property has been used by several authors (see, for example, Siegwarth[20] and Hong[21]) who studied mixed convection in horizontal tube flow for a fluid with $Pr \to \infty$ considering that the axial profile is axisymmetric and parabolic.

Similarly, the effects of natural convection on the intensity of the secondary flow field and on the fluid temperature stratification are more pronounced for air than for water. This observation is corroborated by an examination of the secondary streamlines and isotherms for water (*Figure 5a*) and air (*Figure 5c* of Reference 10) corresponding to $\alpha = 0°$ and $Ra = 7 \times 10^3$. Thus, the intensity of the secondary flow as indicated by the value of ψ_{max} is 7.5 times greater in air than in water, although the position of the vortex centre and the shape of the streamlines is essentially the same for both fluids. Furthermore, the temperature stratification, characterized by the difference $T_{max} - T_{min}$, is considerably higher for air than for water, even though the shape of the isotherms is the same for both fluids.

The fact that these effects are less important in water than in air is due to the simultaneous effects of water's highly viscosity (greater resistance to the establishment of the secondary flow) and lower diffusivity (which restricts the importance of the driving buoyancy force).

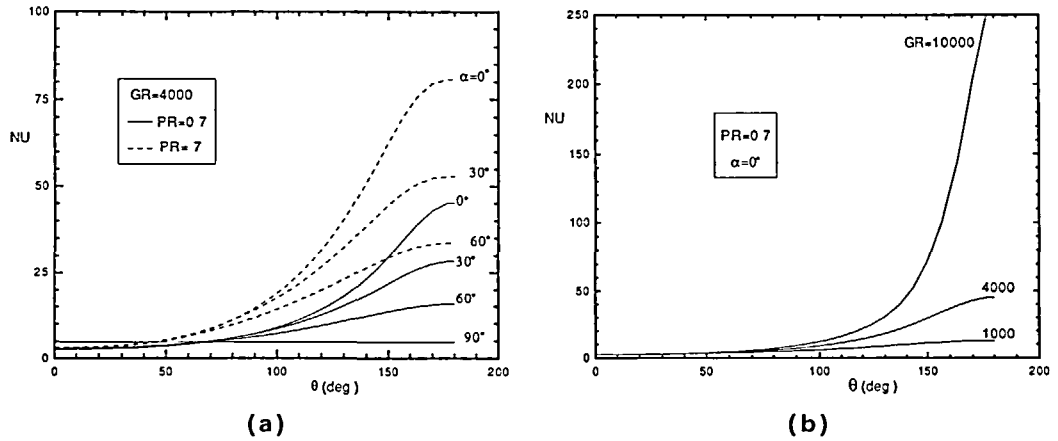

Figure 7 Effect of tube inclination and Grashof number on the circumferential distribution of the local Nusselt number

Local heat transfer coefficient and wall shear stress

Figures 7a and *7b* show respectively the influence of tube inclination and Grashof number on the circumferential distribution of the local Nusselt number (in the chosen adimensionalization scheme $Nu=2/T_w$) for both air and water. For nearly horizontal tubes ($\alpha \leqslant 30°$) Nu varies considerably along the tube perimeter, especially in its lower part where the values are very high, for water in particular. For nearly vertical tubes the circumferential variation disappears since the flow tends to become axisymmetric and the Nusselt number is everywhere higher than the value of 4.36 corresponding to pure forced flow. The influence of the Grashof number on the local heat transfer coefficient is important since the intensity of the secondary flow increases appreciably with Gr, but as shown in *Figure 7b* its effect for horizontal tubes is only evident in the lower part of the tube. This result is consistent with the earlier observation that for horizontal tubes the secondary flow is most significant in the lower part of the tube, especially at high Grashof numbers.

Figure 8a illustrates the effect of tube inclination on the circumferential distribution of the wall shear stress for air and water with $Gr=4000$:

$$\tau=\frac{1}{Re}\left[\frac{\partial V_z}{\partial r}\right]_{r=1} \tag{11a}$$

For the case of air the product $\tau \cdot Re$ varies considerably around the tube perimeter, especially for a horizontal tube. This variation decreases as the tube inclination increases and in the limiting case of a vertical tube a uniform value of $\tau \cdot Re=5.00$ has been obtained. The average wall shear stress:

$$\bar{\tau}=\frac{1}{\pi}\int_0^{\pi} \tau \cdot d\theta \tag{11b}$$

is also dependent on the tube inclination: for $\alpha=0°$, 30°, 60° and 90° the value of $\bar{\tau} \cdot Re$ for air is respectively 4.62, 4.72, 4.80 and 5.00, that is considerably higher than the value of 4.00 corresponding to pure forced flow. For the case of water, the effect of tube inclination on the circumferential distribution of $\tau \cdot Re$ is quite different. Thus, for flow in a horizontal tube with $Gr=4000$, the value of $\tau \cdot Re$ does not vary much around the tube perimeter. As the tube inclination increases, the wall shear stress increases in the upper part of the tube while it decreases in the lower part. However, for the limiting case of the vertical tube a uniform value of $\tau \cdot Re=5.00$

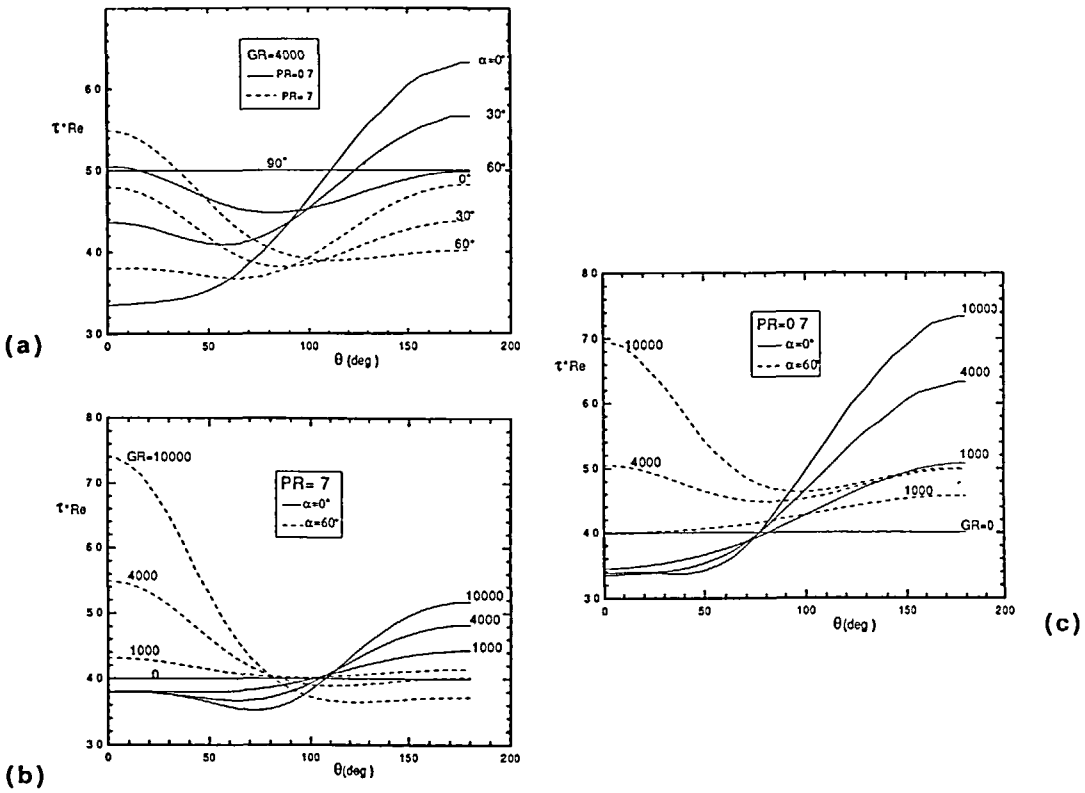

Figure 8 Circumferential distribution of the wall shear stress

(the same as for air) is obtained. The average wall shear stress $\bar{\tau} \cdot Re$ for water is 4.10, 4.24, 4.38 and 5.00 for $\alpha = 0°$, 30°, 60° and 90° respectively. Thus, the effect of tube inclination on the average wall shear stress is qualitatively the same for the two fluids but its quantitative effect is more important in the case of water.

Figures 8b and *8c* show the effect of the Grashof number on the circumferential distribution of the wall shear stress for air and water respectively. For air in horizontal tubes, the effect of θ on $\tau \cdot Re$ is qualitatively the same: for all three non-zero values of Gr we observe an inflexion point at about 80°; in the upper region of the tube ($\theta < 80°$) the local shear stress $\tau \cdot Re$ is lower than 40, the value corresponding to pure forced flow, and the influence of Gr is not significant; in the lower part of the tube ($\theta > 80°$), however, the values of $\tau \cdot Re$ are considerably higher than that corresponding to pure forced flow and increases considerably with Gr. This difference between the upper and lower regions of the tube is, of course, related to the intensity of the secondary flow and the resulting distortion of the axial velocity profile from the axisymmetric Poiseuille distribution. The average value of $\tau \cdot Re$ for horizontal flow of air increases significantly with Gr: its value for $Gr = 0$, 1000, 4000 and 10,000 is 4.00, 4.24, 4.71 and 5.15 respectively. For air in inclined tubes ($\alpha = 60°$) the circumferential distribution of $\tau \cdot Re$ is very different from that in horizontal tubes: its values are always higher than 4.0 and the effect of Gr is more significant in the upper region of the tube. For water (*Figure 8c*) in horizontal tubes the behaviour is similar to that for air but the effect of Gr is less significant, it is interesting to note that for relatively high heat fluxes ($Gr \approx 10{,}000$) a minimum value of $\tau \cdot Re$ is observed at $\theta \approx 75°$. For flow of water in inclined tubes, higher values of $\tau \cdot Re$ occur in the upper region of the tube, as for air; the

difference between the value at the top ($\theta=0$) and the bottom ($\theta=180°$) of the tube is much more important than for air.

Average heat transfer coefficient

Figure 9 shows the effects of the governing parameters *Gr*, *Pr* and α on the average Nusselt number defined as:

$$\overline{Nu}=2/\overline{T_w} \tag{12}$$

where $\overline{T_w}$ is the dimensionless average temperature on the wall perimeter. For a given tube inclination and Grashof number, $\overline{Nu}$ is higher for water than for air except in the case of vertical tubes. Indeed, for $\alpha=90°$, the numerical results confirm the theoretically established property that the flow and thermal fields are independent of the nature of the fluid. Furthermore, the results of *Figure 9* show that for $Gr<10^4$, the average Nusselt number is essentially independent of the tube inclination in the case of air. In the case of water, however, this is only true for $\alpha<60°$ while for nearly vertical tubes the average Grashof number decreases rapidly as α increases. This behaviour has been observed experimentally by Barozzi *et al.*[5]. For high Grashof numbers however, the average Nusselt number increases considerably when α increases from 0° to 30°. It decreases when α increases from 60° to 90° but this effect is much more pronounced for water than for air. The results of *Figure 9* furthermore indicate that when natural convection effects are small (i.e. for small values of *Gr*), $\overline{Nu}$ decreases monotonically as α increases while for larger values of *Gr* there exists a definite optimum inclination for which $\overline{Nu}$ reaches a maximum. This is an important result since it reconciles the apparent contradiction between the analytical prediction of an optimum non-zero inclination by Iqbal and Stachiewicz[6] with the numerical results by Cheng and Hong[8] and, more particularly, with the experimental data of Barozzi *et al.*[5] who did not observe any evidence of such an optimum inclination.

The effect of *Gr* on $\overline{Nu}$ is shown in *Figure 10* for $\alpha=30°$ and both fluids under consideration. Similar results have been obtained for $\alpha=0°$, 60° and 90°. For all these inclinations, the calculated values indicate that for both fluids $\overline{Nu}$ increases monotonically with *Gr* and can be correlated by an expression such as that proposed by:

$$\frac{\overline{Nu}}{Nu_0}=\left(1+\frac{Ra}{A}Pr^b\right)^c=\left(1+\frac{Gr}{A}Pr^{b+1}\right)^c \tag{13}$$

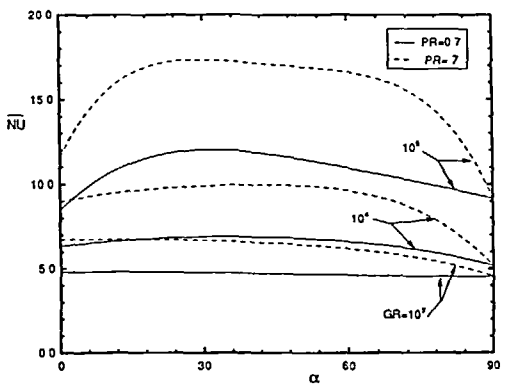

Figure 9 Effect of tube inclination on the average Nusselt number

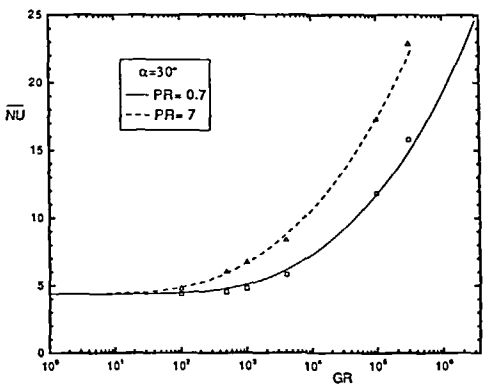

Figure 10 Effect of *Gr* on the average Nusselt number

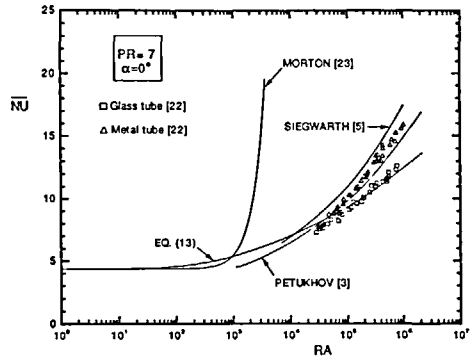

Figure 11 Comparison of proposed correlation with experimental results and other published correlations

Table 2 Constants for the correlation expressing $\overline{Nu}$

Tube inclination	A	b	c
0°	325.6	0.175	0.125
30°	754.1	−0.208	0.215
60°	1038	−0.196	0.219
90°	7500	−1	0.270

where $Nu_0 = 4.364$ is the Nusselt number for pure forced flow with uniform heat flux at the wall. The constants A, b and c depend on the tube inclination. Their values, calculated by using the least-squares curve-fitting technique from the numerical results obtained with $Re = 250$ and $Ra \leqslant 2.1 \times 10^6$, are given in *Table 2*. The correlations for $\alpha = 30°$ are also shown in *Figure 10*.

Finally, *Figure 11* provides a comparison of the proposed correlation for water flow in horizontal tubes with the experimental results of Morcos[22] and with previously published correlations. The correlation attributed to Morton by Mori[23] was obtained by a perturbation technique and is obviously valid only for very small Grashof numbers. The correlation attributed to Siegwarth by Barozzi[5] as well as the one proposed by Petukhov and Polyakov[3] are in good agreement with the experimental results for metal tubes while our correlation is in better agreement with the experimental values measured in glass tubes. This is to be expected since experimentally developed correlations are obtained with the heat flux condition applied on the outside surface of the tube: for metal tubes with high conductivity, the resulting thermal condition on the interior surface (at $r = 1$) is closer to a uniform temperature while for tubes with low conductivity (such as glass tubes) the thermal condition at $r = 1$ is closer to the uniform thermal flux condition used in the present numerical study. Therefore our numerical results calculated with a uniform heat flux condition at the fluid–solid interface, correspond to the experimental values measured by Morcos in glass tubes: their close agreement is a clear indication of the accuracy of the model and the precision of the numerical technique used in this study.

CONCLUSION

In this study, the effect of natural convection on the fully developed laminar upward flow in an inclined uniformly heated tube has been numerically investigated. The results have shown that

the effects of the buoyancy induced secondary flow on the hydrodynamic and thermal fields are very complex and strongly dependent on the Grashof number, the Prandtl number and the tube inclination. In particular it has been shown that:

—the intensity of the secondary flow is greater for air than for water, decreases as the tube inclination increases and increases with the Grashof number;
—the distortion of the axial velocity profile and of the temperature field from the corresponding distributions for pure forced flow is greater for air than for water and increases with the Grashof number;
—the local Nusselt number for low tube inclinations varies considerably along the tube perimeter for both fluids and is very different from the value corresponding to pure forced flow; the difference between its extreme values increases with the Grashof number;
—the local shear stress varies considerably along the tube perimeter; the difference between its extreme values is higher for air than for water;
—the average shear stress is higher for air than for water and increases with tube inclination and with the Grashof number;
—the average Nusselt number increases with the Grashof number for both fluids and any tube inclination; for a given fluid and Grashof number there exists an optimum tube inclination which maximizes the average Nusselt number (at very low Grashof numbers the maximum Nusselt numbers occurs for horizontal tube); for a given inclination and Grashof number, the average Nusselt number for water is higher than the one for air.

Appropriate correlations for the average Nusselt number in terms of Gr and Pr have been obtained for four different tube inclinations ($\alpha = 0°$, 30°, 60° and 90°).

ACKNOWLEDGEMENTS

The authors wish to thank the Natural Sciences and Engineering Research Council of Canada and the 'Fonds FCAR du Québec' for their financial support as well as Université de Sherbrooke and Université de Moncton for computing time allocation.

REFERENCES

1 Nguyen, C. T. and Galanis, N. Combined forced and free convection for the developing laminar flow in horizontal tubes under uniform heat flux, *Numerical Methods in Thermal Problems*, Vol. 5, Pineridge Press, Swansea, Part 1 (1987)
2 Nguyen, C. T. and Galanis, N. Investigation of Rayleigh number effects on combined forced and free convection for developing laminar flow in uniformly heated horizontal tubes, *ASHRAE Trans.* **95**, (1), 171–178 (1989)
3 Petukhov, B. S. and Polyakov, A. F. Experimental investigation of viscogravitational fluid flow in a horizontal tube, Sci. Res. Inst. of High Temp. [Transl. *Teplofizika Vysokikh Temperatur*, **5**, 87–95 (1967)]
4 Petukhov B. S. *et al.*, Heat transfer in tubes with viscous-gravity flow, *Heat Transfer-Soviet Res.* **1**, 24–31 (1969)
5 Barozzi, G. S. *et al.*, Experimental investigation of combined forced and free convection in horizontal and inclined tubes, *Meccanica*, **20**, 18–27 (1985)
6 Iqbal, M. and Stachiewicz, J. W. Influence of tube orientation on combined free and forced laminar convection heat transfer, *Trans. ASME, J. Heat Transf.* **88**, 109–116 (1966)
7 Hong, S. W. and Bergles, A. E. Theoretical solution for combined forced and free convection in horizontal tubes with temperature-dependent viscosity, *Trans. ASME, J. Heat Transf.* **98**, 459–465 (1976)
8 Cheng, K. C. and Hong, S. W. Combined free and forced laminar convection in inclined tubes, *Appl. Sci. Res.*, **27**, 19–38 (1972)
9 Orfi, J., Galanis, N. and Nguyen, C. T. Laminar incompressible flow with mixed convection in inclined tubes, *Proc. IASTED Int. Symp. Modelling, Simulation and Optimization, Montreal.* ACTA Press, pp. 127–130 (1990)
10 Orfi, J., Galanis, N. and Nguyen, C. T. Mixed convection for the fully-developed laminar flow in inclined uniformly heated tubes, *Numerical Methods in Thermal Problems*, Vol. VIII, Pineridge Press, Swansea, Pt. 1 (1991)
11 Patankar, S. V. and Spalding, C. B. A calculation procedure for heat, mass and momentum transfer in three-dimensional parabolic flows, *Int. J. Heat Mass Transfer*, **15**, 1787–1806 (1972)
12 Rustum, I. M. and Soliman, H. M. Numerical analysis of laminar mixed convection in horizontal internally finned tubes, *Int. J. Heat Mass Transfer*, **33**, 1485–1496 (1990)

13 Nieckele, A. O. and Patankar, S. V. Laminar mixed convection in a concentric annulus with horizontal axis, *Trans. ASME, J. Heat Transf.*, **107**, 902–908 (1985)
14 Patankar, S. V. *Numerical Heat Transfer and Fluid Flow*, Hemisphere & McGraw-Hill, New York (1980)
15 Orfi, J. Étude de l'effet de la convection naturelle sur un écoulement laminaire développé dans un tuyau incliné chauffé uniformément à la paroi, *Mémoire MScA*, Univ. de Sherbrooke (1991)
16 Nguyen, C. T. Convection mixte en régime laminaire dans un tuyau incliné soumis à un flux de chaleur constant à la paroi, *Thèse PhD*, Univ. de Sherbrooke (1988)
17 Collins, M. W. Combined convection in vertical tubes, heat and mass transfer by combined forced and natural convection, *Inst. Mech. Eng. Symp. Paper no. C115-71, Manchester*, pp. 17–25 (1971)
18 Petukhov, B. S. and Polyakov, A. F. Effect of free convection on heat transfer during forced flow in a horizontal pipe, *High Temp. Res. Inst.*, **5**, 348–351 (1967)
19 Newel, Jr., P. and Bergles, A. E. Analysis of combined free and forced convection for fully developed laminar flow in horizontal tubes, *Trans. ASME, J. Heat Transf.*, **92**, 83–93 (1970)
20 Siegwarth, D. P. *et al.* Effect of secondary flow on the temperature and primary flow in a heated horizontal tube, *Int. J. Heat Mass Transfer*, **12**, 1535–1551 (1969)
21 Hong, S. W. Laminar flow heat transfer in ordinary and augmented tubes, *PhD Thesis*, Iowa State University, p. 273 (1974)
22 Morcos, S. M. Combined forced and free laminar convection in horizontal tubes, *PhD Thesis*, Iowa State University, p. 152 (1974)
23 Mori Y. *et al.* Forced convective heat transfer in uniformly heated horizontal tubes, 1st Report—Experimental Study on the Effect of Buoyancy, *Int. J. Heat Mass Transfer*, **9**, 453–463 (1966)